Theoretical study of the phase transformations of $Sr_3Hf_2O_7$

E. Lora da Silva[1*], A. Mokhles Gerami[2,3], P. Neenu Lekshmi,[1] J. G. M. Correia,[4,3] J. P. Araujo,[1] A. M. L Lopes[1]

[1] IFIMUP, Department of Physics and Astronomy, Faculty of Sciences, University of Porto, Porto, Portugal
[2] School of Particles and Accelerators, Institute for Research in Fundamental Sciences (IPM), Tehran, Iran
[3] CERN, Esplanade des Particules 1, Geneva 23, Switzerland
[4] C2TN, Departamento de Engenharia e Ciências Nucleares, Instituto Superior Técnico, Universidade de Lisboa, Bobadela LRS, Portugal

I. Aim

We present an *ab-initio* study performed by means of Density Functional Theory (DFT), group-subgroup symmetry analysis and lattice dynamics to direct the design of Ruddelstein-Popper (RP) perovskite systems with novel properties and therefore aid experimental synthesis. From this study it is possible to obtain information regarding the structural properties and local landscapes, such as octahedra rotations, tilts and distortions which occur during a structural phase transition, and that will aid and complement the interpretation of analysis performed through Perturbed Angular Correlation (PAC) radioactive nuclear techniques. More specifically we focus our study on the Sr_3Hf_2O7 system characterized by a high-temperature *I4/mmm* (S.G. 139) centrosymmetric structure and a ground-state $Cmc2_1$ (S. G. 36) ferroelectric system. We have probed potential candidates that may form the pathway transition through the *I4/mmm* → $Cmc2_1$ the structural phase transitions, and which were obtained through group-theoretical analysis.

II. Theoretical Methodology

- Density Functional Theory by employing the semi-local generalized-gradient approximation functional with the Perdew-Burke-Ernzerhof parametrisation revised for solids (PBEsol) [1]
- Quantum Espresso (QE) [2]: structural relaxations and lattice dynamics calculations
  - Projector augmented-wave (PAW) [3] with Sr[$4s^24p^65s^2$], Hf[$5s^25p^65d^26s^2$] and O[$2s^22p^4$] electrons
  - Plane-wave kinetic-energy cut-off of 70 Ry
  - Sampling of Brillouin-Zone (BZ): Γ-centred Monkhorst-Pack [4] mesh12x12x6 subdivisions
  - Lattice dynamics implemented in Phonopy package [5] (finite displacement method employed on a 2*x*2*x*2 supercell and phonon frequencies sampled on an interpolated **q**-point mesh of 50x50x50)
- WIEN2K [6]: Band gaps, Electric field gradients (EFG), and Macroscopic polarization
  - Radii of the muffin-tin atomic spheres: Sr, Hf, and O are set to 2.25, 2.07, and 1.78 a.u., respectively
  - -6 Ry is set as the boundary separating the core electron states and valence electron states
  - Cut-off parameter RMT×KMAX : 6.0 (a.u.)$^{-1}$
  - The G_{max}, Fourier expansion of the charge density, is restricted to 16 (Ry)$^{1/2}$
  - Mesh of (6×6×6) **k**-points applied for the sampling of the irreducible first BZ
  - Meta-GGA functional, the modified Becke-Johnson approximation (mBJ) [7], applied to obtain more reliable band-gap energies

III. Results and Discussion

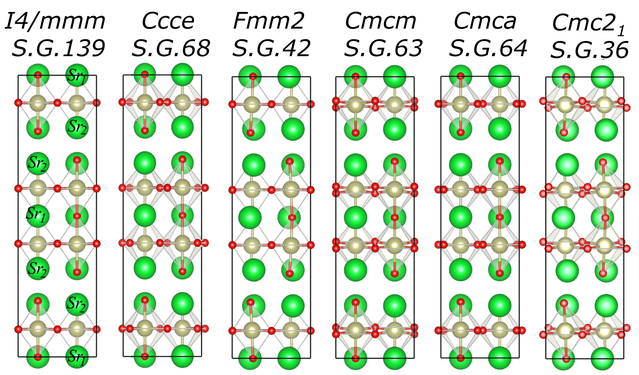

Figure 1 (top): Representation of the different structural phases of $Sr_3Hf_2O_7$, namely the parent *I4/mmm* structure, intermediate pathway structural phases and the ground-state $Cmc2_1$ system (ordered by energetic stability with respect to the ground-state $Cmc2_1$ system. O ions are shown in red, Sr in green and Hf in gold.

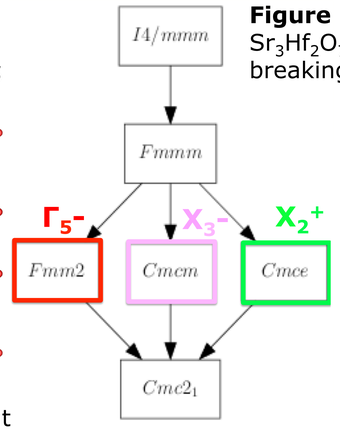

Figure 2 (left): Barnighausen tree for the group-subgroup relationship between the aristotype *I4/mmm* and $Cmc2_1$ ground-state $Sr_3Hf_2O_7$ structures. The ir.rep. labels indicate the distortion components and related isotropy group that contribute to the symmetry-breaking of *I4/mmm* → $Cmc2_1$ The graph was obtained using the SYMMODES software [8].

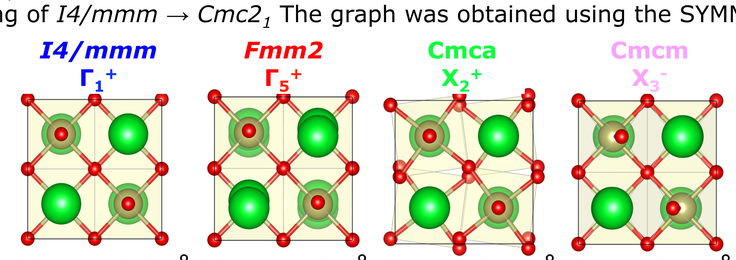

Figure 3 (left): Decomposition of the structural distortion from *I4/mmm* → $Cmc2_1$ into contributions from lattice modes with different symmetries obtained by employing AMPLIMODES [9]. The distorted structure derives from the high-symmetry structure through four frozen distortions, Γ_1^+, Γ_5^-, X_2^+ and X_3^-.

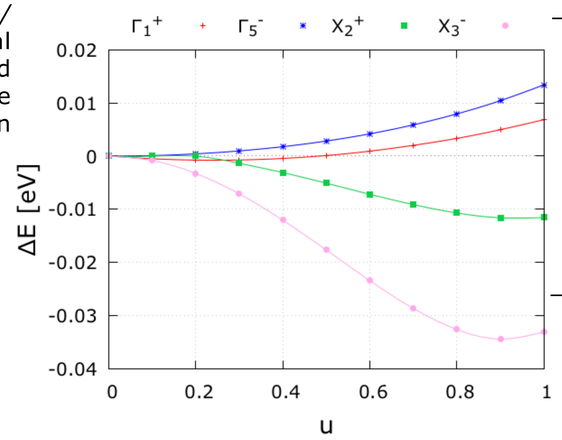

Figure 4 (right): Potential energy surface along each distortion mode, with u = 0 being the centrosymmetric tetragonal structure and u = 1 the distortion structure corresponding to the isotropy sub-group of the frozen mode. All the four distortion modes contribute to the $Cmc2_1$ distortion, although the most significant distortions are related to the X_2^+ and X_3^- modes.

Space Group	Sr_1		Sr_2		Hf	
	V_{zz} (V/Å^2)	η	V_{zz} (V/Å^2)	η	V_{zz} (V/Å^2)	η
I4/mmm	11.84	0.000	-77.91	0.000	16.38	0.000
Ccce	-58.21	0.001	-90.77	0.672	72.37	0.010
Fmm2	11.60	0.011	-76.44	0.000	20.15	0.037
Cmcm	-41.54	0.724	-54.48	0.769	48.87	0.701
Cmca	74.21	0.163	-119.55	0.606	-89.63	0.129
$Cmc2_1$	-43.79	0.731	-58.31	0.955	37.18	0.408

Table 1 (top): Calculated electric field gradients (V_{zz}) and asymmetric parameter (η) of the Sr_1, Sr_2 and Hf sites of the different structural phases of $Sr_3Hf_2O_7$.

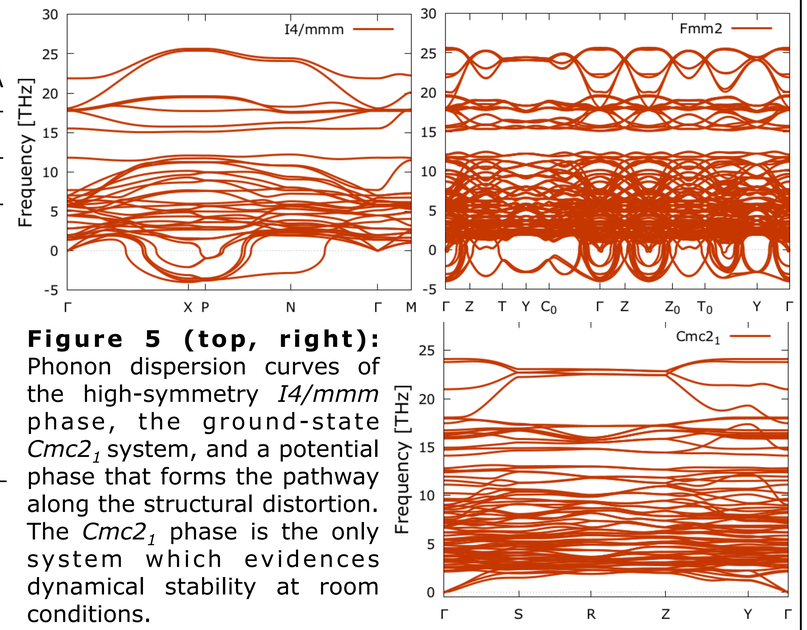

Figure 5 (top, right): Phonon dispersion curves of the high-symmetry *I4/mmm* phase, the ground-state $Cmc2_1$ system, and a potential phase that forms the pathway along the structural distortion. The $Cmc2_1$ phase is the only system which evidences dynamical stability at room conditions.

V. References

[1] J. P. Perdew, *et al*, Phys. Rev. Lett. 100, 136406 (2008). J. P. Perdew, *et al*, Phys. Rev. Lett. 102, 039902(E) (2009). **[2]** P. Giannozzi, *et al*. J.Phys.:Condens.Matter 21, 395502 (2009). P. Giannozzi, *et al.*, J.Phys.:Condens.Matter 29, 465901 (2017). P. Giannozzi, *et al*., J. Chem. Phys. 152:154105, 2020. **[3]** P. E. Blochl, Phys. Rev. B 50, 17953 (1994). **[4]** H. J. Monkhorst and J. D. Pack, Phys. Rev. B 13, 5188 (1976). **[5]** Togo and Tanaka, Scr. Mater. 108, 1 (2015). **[6]** P. Blaha, et al., J. Chem. Phys. 152, 074101 (2020). **[7]** F. Tran and P. Blaha, Phys. Rev. Lett. 102, 226401 (2009). **[8]** Symmmodes. http://www.cryst.ehu.es/cryst/symmodes.html. **[9]** Amplimodes. http://www.cryst.ehu.es/cryst/amplimodes.html.

VI. Acknowledgements

This research was supported by the project NECL under NORTE-01-0145-FEDER-022096, POCI-01-0145-FEDER-029454, POCI-01-0145-FEDER-032527, and CERN/FIS-PAR/0005/2017. The authors acknowledge computing resources from PRACE Project Access, Call 20 (FLIP Project 02/SAICT/2017-029454) with technical support provided by CINECA and the cluster resources provided by CERN (HTCondor).

*estelina.silva@ifc.up.pt